Iris Recognition

Part I: Patrick Gampp
Part II: Andrea Sereinig

Advanced Signal Processing Seminar

Graz, 12/05/2007

Content

- Part I:
  - Basics
  - The Daugman Iris Recognition System
- Part II:
  - Wildes Iris Recognition
  - Iris on the Move
  - Iris Recognition Systems

Part I: Content

- Motivation
- Anatomy of the Human Iris
- Image Aquisition
- Iris Localization
- Wavelet Transformation
- Iris Feature Encoding by 2D Wavelets Demodulation
- Pattern Matching
- Recognizing Irises Regardless of Size, Position and Orientation
- Decision Environment
- Countermeasures Against Subterfuge
- Performance, Execution Speed

Motivation

- Noninvasive
- Covert evaluation possible
- Iris patterns variability is enormous
- Iris is well protected from environment
- Iris pattern is stable over time
- Insensitive to angle of illumination
- Insensitive to changes in viewing

Anatomy of the Human Iris (1)

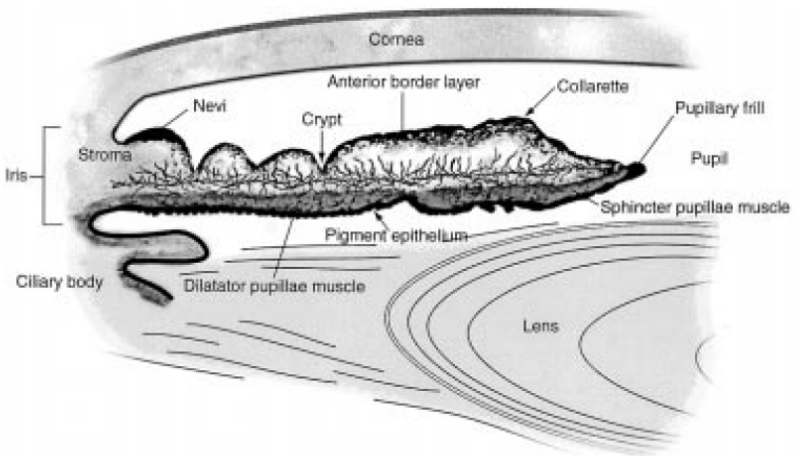

[Wildes 1997]

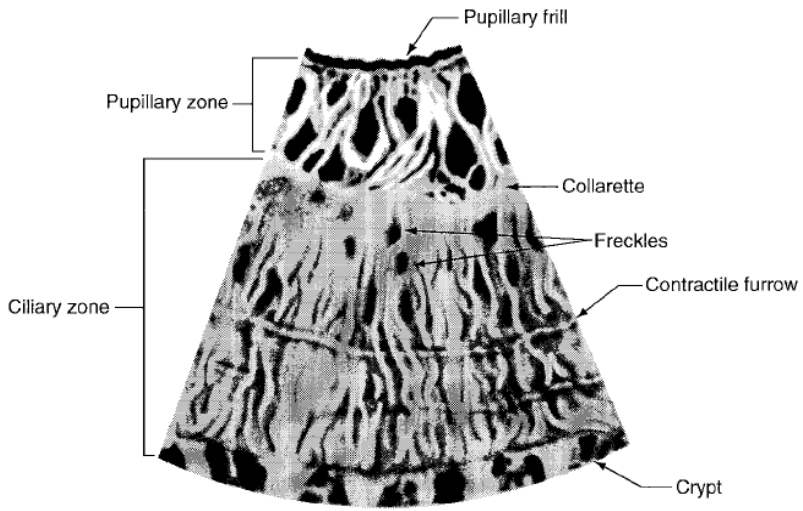

[Wildes 1997]

Anatomy of the Human Iris (2)

- Iris patterns largely complete by eighth month
- Pigmentation accretion into adolescence
- Average pupil size increases until adolescence
- Advanced age: slight depigmentation and shrinking of pupillary opening
- Patterns are stable with age
- General structure genetically determined, but minutiae dependend from initial conditions
- NIR wavelengths reveal deeper stromal features

Image Aquisition (1)

- Need sufficient resolution, sharpness, contrast
- Iris is relatively small
- Iris is dark object
- Human operators are sensitive about their eyes
- Well-centered image while remaining noninvasive
- Eliminate artifacts like reflectations, aberrations

Image Aquisition (2)

- LED point light source
- NIR illumination 700nm- 900nm
- Sensitive CCD camera
- 100- 200 pixels monochromatic image
- Distance 15- 46cm
- Video rate capture
- Self- positioning of object
- Focus assessment: maximizing high-frequency power of 2D Fourier spectrum

Iris Localization

1. Cirular path of contour integration for pupil edge
2. Circular path for limbic boundaries
3. Arcuate path with fitted splines for eyelid boundaries

$$\max_{(r,x_0,y_0)} \left| G_\sigma(r) * \frac{\partial}{\partial r} \oint_{(r,x_0,y_0)} \frac{I(x,y)}{2\pi r} ds \right|$$

$$G(r)_\sigma = \frac{1}{\sigma\sqrt{2\pi}} e^{-\left(\frac{(r-r_0)^2}{2\sigma^2}\right)}$$

$I(x,y)$....., Image

r....., Radius

(x_0, y_0)....., Center Coordinates

$G_\sigma(r)$....., Gaussian smoothing function

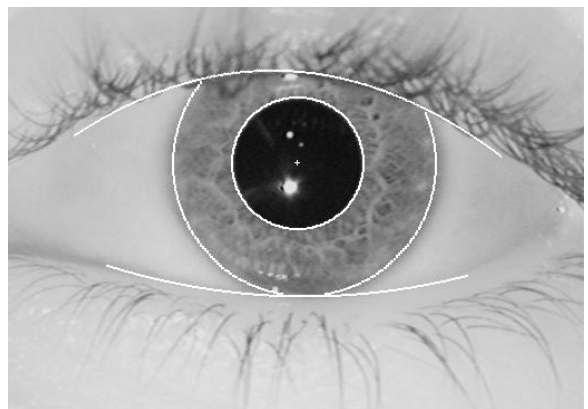

[Daugman Website]

Why (Gabor) Wavelets?

- Advantage over Fourier Transform representing functions with discontinuities and sharp peaks
- Compact representation of images, eg. jpeg2000

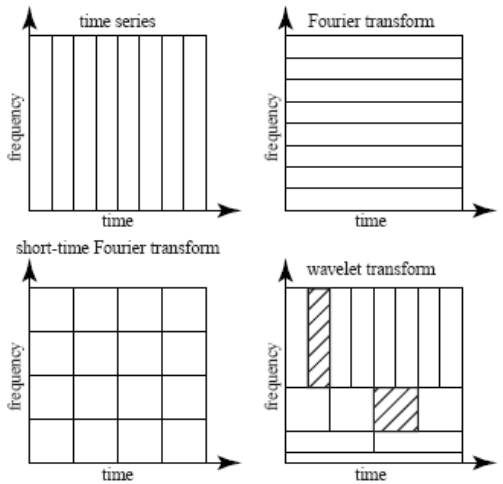

[Ulrich Günther 2001]

- Simple cells in visual cortex can be modelled
- „Quantum principle“ in information
  → good time- vs. frequency- resolution trade-off

Complex 2D Gabor Wavelets

- Mother function:

$$\Psi(x,y) = e^{-2\pi i[u_0(x-x_0)+v_0(y-y_0)]} e^{-\pi\left[\frac{(x-x_0)^2}{\alpha^2}+\frac{(y-y_0)^2}{\beta^2}\right]}$$

- Generating function:

$$\Psi_{mpq\theta}(x,y) = 2^{-2m}\Psi(x',y')$$

$$x' = 2^{-m}[x\cos(\theta) + y\sin(\theta)] - p$$
$$y' = 2^{-m}[-x\sin(\theta) + y\sin(\theta)] - q$$

x_0, y_0....., Location of peak of gaussian envelope
x, y....., Visual space variables
α, β....., Width and Length of envelope
u_0, v_0....., Spatial frequency variables of sinusoidal carrier
θ....., Discrete rotation of envelope
m....., Dilation parameter
p, q....., Translation in position; shift parameters

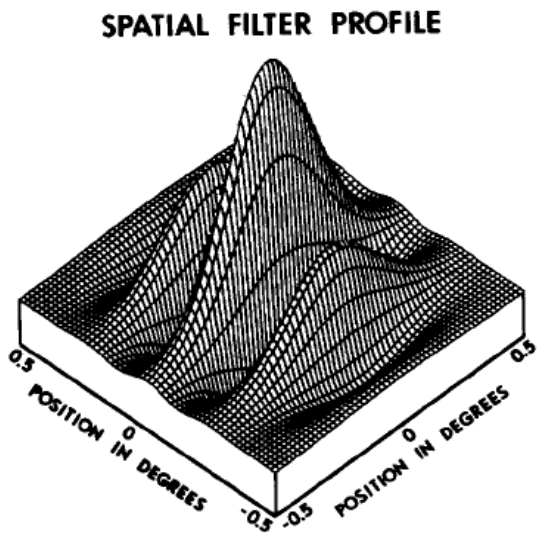

[Daugman 1988]

Iris Pattern Encoding (1)

$$h_{\mathrm{Re}} = \begin{cases} 1, if\ \mathrm{Re}\left\{\int_{\rho}\int_{\phi} I(\rho,\phi) e^{-i\omega(\theta_0-\phi)} e^{\frac{-(r_0-\rho)^2}{\alpha^2}} e^{\frac{-(\theta_0-\phi)^2}{\beta^2}} \rho d\rho d\phi\right\} \geq 0 \\ 0, if\ \mathrm{Re}\left\{\int_{\rho}\int_{\phi} I(\rho,\phi) e^{-i\omega(\theta_0-\phi)} e^{\frac{-(r_0-\rho)^2}{\alpha^2}} e^{\frac{-(\theta_0-\phi)^2}{\beta^2}} \rho d\rho d\phi\right\} \prec 0 \end{cases}$$

$$h_{\mathrm{Im}} = \begin{cases} 1, if\ \mathrm{Im}\left\{\int_{\rho}\int_{\phi} I(\rho,\phi) e^{-i\omega(\theta_0-\phi)} e^{\frac{-(r_0-\rho)^2}{\alpha^2}} e^{\frac{-(\theta_0-\phi)^2}{\beta^2}} \rho d\rho d\phi\right\} \geq 0 \\ 0, if\ \mathrm{Im}\left\{\int_{\rho}\int_{\phi} I(\rho,\phi) e^{-i\omega(\theta_0-\phi)} e^{\frac{-(r_0-\rho)^2}{\alpha^2}} e^{\frac{-(\theta_0-\phi)^2}{\beta^2}} \rho d\rho d\phi\right\} \prec 0 \end{cases}$$

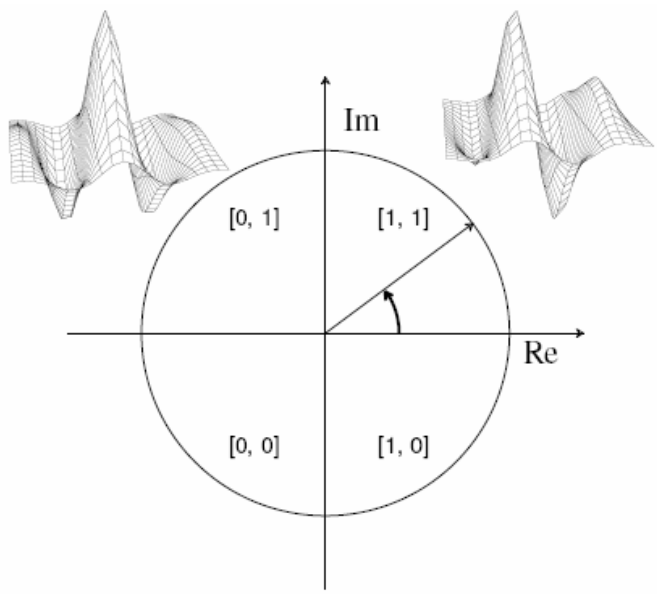

[Daugman Website]

I(ρ, φ)....., Raw iris image in polar coordinate system

α, β....., Multi - scale wavelet size parameters; 8 - fold range from 0.15mm to 1.2mm

ω....., Wavelet frequency; spanning 3 octaves inverse proportion to β

r_0, θ_0....., Iris region

Iris Pattern Encoding (2)

- Cyclic phase- quadrant code: Gray code
- Coarse phase quadrant quantization:
  → Ignore imaging contrast, illumination, camera gain
- Many wavelet sizes, frequencies, orientations
  → 256 Byte per iris
- Masking bits: ignore obscured data

Pattern Matching

- Test of statistical independence
- Fractional HD (Hamming Distance)

$$HD = \frac{\left\| (\text{code A} \otimes \text{code B}) \cap \text{mask A} \cap \text{mask B} \right\|}{\left\| \text{mask A} \cap \text{mask B} \right\|}$$

- Obscured data: set mask bit ‚0‘
- XOR, AND in parallel wordlength- size chunks
  → single machine instruction
- 300MHz CPU: 100 000 iris comparisons per second

Distribution of Hamming Distances

- 9 million comparisons of different irises
- 4258 iris images acquired in UK, USA, Japan, Korea
- Bernoulli trial, but correlation between „coin tosses“
- Only small subsets of bits are mutually independent
- Same distribution for genetically identical irises

$$f(m) = \binom{N}{m} p^m (1-p)^{(N-m)}$$

$$\sigma^2 = \frac{p(1-p)}{N} \text{ (for correlated Bernoulli trials)}$$

$$\Rightarrow N = 249 \text{ Degrees of freedom}$$

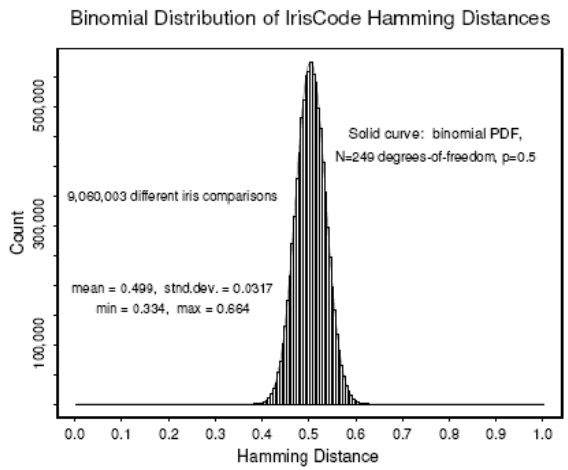

[Daugman 2004]

Homogeneous Rubber Sheet Model

- Problem: Pupil size change
- Solution:

$$I\big(x(r,\theta), y(r,\theta)\big) \rightarrow I(r,\theta)$$
$$r \in [0,1]$$
$$\theta \in [0,2\pi]$$

$$\boxed{\begin{aligned} x(r,\theta) &= (1-r)x_p(\theta) + r x_s(\theta) \\ y(r,\theta) &= (1-r)y_p(\theta) + r y_s(\theta) \end{aligned}}$$

$(x_s(\theta), y_s(\theta))$....., Limbus boundary points
$(x_p(\theta), y_p(\theta))$....., Pupillary boundary points

Cyclic Scrolling

- Problem: Iris orientation depends upon head tilt etc
- Solution: Compare iris code at many orientations
- Preserve only best match

$$F_n(x) = 1 - [1 - F_0(x)]^n$$

$$f_n(x) = \frac{d}{dx} F_n(x) = n f_0(x) [1 - F_0(x)]^{n-1}$$

f_0 ....., PDF for comparison in 1 orientation

$F_0(x)$ ....., CDF

x....., HD Acceptance Criterion

$F_0(x) = \int_0^x f_0(x)dx$ ....., Probability of getting a false match

$1 - F_0(x)$ ....., Probability of not getting false match

$[1 - F_0(x)]^n$ ....., n independent tests at n relative orientations

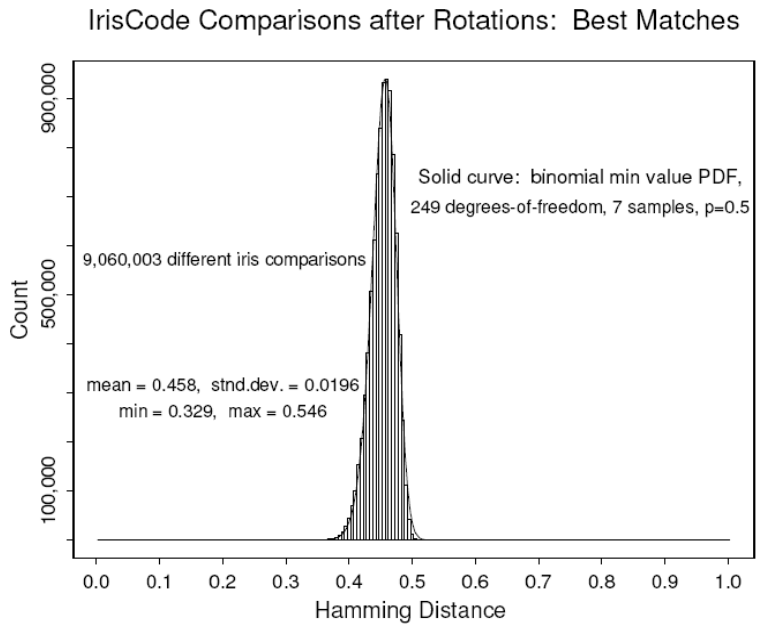

[Daugman 2004]

Uniqueness of Failing the Test of Statistical Independence

- Cumulative binomial distribution function

$$F_n(x) = \sum_{x=0}^{x} f_n(x)$$

- False match probabilities:

Stirling's Approximation for high factorials

$$n! \approx e^{n\ln(n)-n+\frac{1}{2}\ln(2\pi n)}$$

HD Criterion	*Odds of False Match*
0.26	1 in 10^{13}
0.27	1 in 10^{12}
0.28	1 in 10^{11}
0.29	1 in 13 billion
0.30	1 in 1.5 billion
0.31	1 in 185 million
0.32	1 in 26 million
0.33	1 in 4 million
0.34	1 in 690,000
0.35	1 in 133,000

[Daugman 2004]

→ even poor match (HD=0.3) provides compelling evidence of identity

Decision Environment

- 7070 different pairs of same-eye images
- Overlap between distributions: error rate
- Non-ideal: different distances, cameras, lighting
- Decidability d´: Separation of distributions

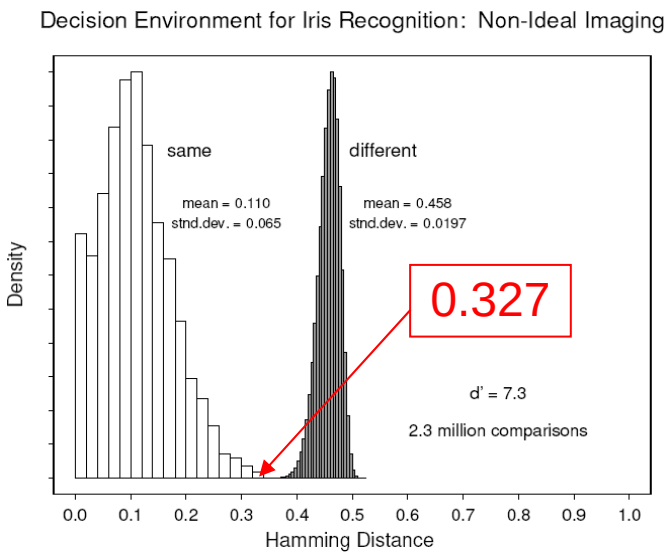

[Daugman 2004]

$$d' = \frac{|\mu_1 - \mu_2|}{\sqrt{\frac{\sigma_1^2 + \sigma_2^2}{2}}}$$

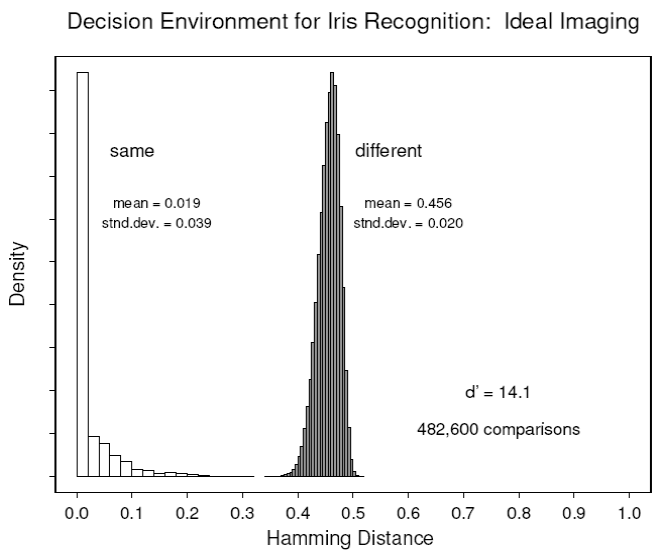

[Daugman 2004]

Countermeasures Against Subterfuge

- Fake iris, photograph, videotape, glass eye….
- Observe pupil diameter caused by random light levels: 250ms constriction, 400ms dilation
- Steady- state oscillation: 0,5Hz (Hippus)
- Track eyelid movements
- Ocular reflection by random light at various positions due to moist cornea
- Spectral signature of living tissue in NIR light
- Vein patterns silhouettes in NIR light

Speed Performance

- 300 Mhz Sun Workstation
- 100 000 iris comparisons per second
- Large database: division into units of 100 000

Operation	*Time*
Assess image focus	15 msec
Scrub specular reflections	56 msec
Localize eye and iris	90 msec
Fit pupillary boundary	12 msec
Detect and fit both eyelids	93 msec
Remove lashes and contact lens edges	78 msec
Demodulation and IrisCode creation	102 msec
XOR comparison of two IrisCodes	10 μs

[Daugman 2004]

References

- [Daugman 2004]: How Iris Recognition Works
- [Wildes 1997]: Iris Recognition: An Emerging Biometric Technology
- [Daugman]: Recognizing Persons by their Iris Patterns
- [Daugman 2003]: Demodulation by Complex- Valued Wavelets for Stochastic Pattern Recognition
- [Daugman 1988]: Complete Discrete 2-D Gabor Transforms by Neural Networks for Image Analysis and Compression
- [Tai Sing Lee 1996]: Image Representation Using 2D Gabor Wavelets
- [Daugman Website]: http://www.cl.cam.ac.uk/~jgd1000/
- [Ulrich Günther 2001]: Advanced Computing in NMR Spectroscopy